Reliability Improvement Approach Based on Flatness Control of Parallel-Connected Inverters

Ahmed Shahin, *Senior Member, IEEE*, Hassan Moussa, *Member, IEEE*, Ivano Forrisi, Jean-Philippe Martin, Babak Nahid-Mobarakeh, *Senior Member, IEEE*, and Serge Pierfederici

***Abstract*—In this paper, a global study in terms of control architecture is applied to parallel voltage-source inverters. Parallelism of inverters represents very interesting advantages for the industrial applications to meet the high-power requirements, and it is possible to apply maintenance during the operation without interruptible operation. The main objective of this paper is to guarantee a reliable operation of the parallel inverters system during healthy and faulty conditions due to full disconnection of any inverter. Special precautions are recommended to avoid the negative effects of the circulating currents, which are caused essentially by the asynchronous pulse width modulation or existence of dispersion of the system component characteristics. To deal with this crucial problem, one-loop flatness-based control is proposed to the control of *N* parallel inverters and allows obtaining low total harmonic distortion. The proposed control uses the advantages of the flatness to ensure high power quality at the point of common coupling and equal currents distribution between the parallel inverters and minimize the impact of a full disconnection of any inverter on the performance. The proposed algorithm is theoretically analyzed and validated experimentally.**

***Index Terms*—Circulating currents, fault impact minimization, flatness control, parallel inverters, reliable operation.**

I. Introduction

THE parallel connection of three-phase inverters is used to increase the system capacity. It is a well-known solution for large-scale inverter systems when the capacities of the switching devices are limited or constrained by economic considerations [1]. For many applications, the parallelism could be crucial in systems with high reliability requirements such as machine drive systems [2], rectifiers [3], and distributed generation systems [4]. Paralleling inverters allow reducing the components size especially the inductive components by segmenting the total power at the point of common coupling (PCC). The global efficiency becomes better and the voltage stress on each inverter can be reduced. Then, the number of the parallel inverters in terms of reliability and cost optimization can be achieved [5], [6].

This leads to enhance reliability of the system, guarantee continuity of the service, and allow possible reconfiguration when one module or more present malfunctioning [7]. The parallel systems allow creating redundancy, achieving compact design, high power density compared to single large power inverter, and making the load power expansion between the parallel inverters more flexible [7]–[11].

The parallelism of the inverters enables current ripple reduction and reduces the size of the output filter or the used transformers [12]–[14]. The major concern for the parallel operation is the circulating current problem through the conduction paths resulting at the common connection of the dc-to-ac terminals of each inverter. Definition of the phenomenon is detailed in [15]–[21]; the circulating currents consist of not only the zero-sequence, but the nonzero-sequence components. There are many reasons of the circulating currents in the parallel inverter system, like the asynchronous switching operation of the individual inverter or due to nonidentical components or open circuit of any switch or at the moment of fully disconnection of any inverter. These currents can be separated into two types: a low-frequency component close to the fundamental frequency and a high-frequency component close to the switching frequency [20], [21]. The high-frequency component can be effectively limited by means of passive components, while the low-frequency component needs a special attention. Traditionally, in order to avoid this problem, the transformers can be used to isolate the direct current flow [22], [23].

However, the transformers are heavy and increase the core and copper losses. Commonly, the recommended solutions in the literature are based on modification of the PWM operation [15], [21]. Other works propose association of the modified switching techniques [24]–[28]. For example, an improved PWM is associated with intercell transformers (ICT) for the case of two inverters [24]. The ICTs allow the current ripple reduction compared to simple inductor filters, but the real practical realization of such solution in the case of *N* units is very complex. A comparative analysis between PWM, SPWM, and DPWM has showed that the SPWM is the best candidate for the parallel inverters with a common dc bus [25]–[27]. An analytical method for reducing the circulating current in the parallel inverters system with SPWM for ac motor drive is detailed in [28], where the driving current and circulating current are modeled by the voltage equations of the inverters and motor load. Many applications detailed the flatness based control. In [29]–[40], this control method is applied to the control of dc-to-dc converters and dc-to-ac inverters for the regulation of the output voltage or power

Manuscript received May 27, 2015; revised October 29, 2015 and January 7, 2016; accepted February 2, 2016. Date of publication February 11, 2016; date of current version September 16, 2016. Recommended for publication by Associate Editor M. Ordonez.

A. Shahin is with the Department of Electrical Engineering, Faculty of Engineering, Mansoura University, Mansoura 35516, Egypt, and also with the GREEN Laboratory, Université de Lorraine, Nancy 54516, France (e-mail: ahmed.shahin@univ-lorraine.fr).

H. Moussa, I. Forrisi, B. Nahid-Mobarakeh, and S. Pierfederici are with the GREEN Laboratory, Université de Lorraine, Vandoeuvre-les-Nancy 54516, France (e-mail: hassan.moussa@univ-lorraine.fr; ivano.forrisi@univ-lorraine.fr; babak.nahidmobarakeh@univ-lorraine.fr; serge.pierfederici@univ-lorraine.fr).

J.-P. Martin is with the Institut National Polytechnique de Lorraine, Vandoeuvre-les-Nancy 54005, France, and also with GREEN Laboratory, Université de Lorraine, Vandoeuvre-les-Nancy 54516, France (e-mail: jean-philippe.martin@univ-lorraine.fr).

Color versions of one or more of the figures in this paper are available online at http://ieeexplore.ieee.org.

Digital Object Identifier 10.1109/TPEL.2016.2527778

by taking in considerations the constraints of the input source like the fuel cells [32]. This kind of control can exhibit more stable operation in the transient conditions compared to the traditional methods for many applications like electric vehicles and power generation systems [31]–[35]. In addition, this method is applied to drive electric machines [33], where the flatness has been exploited for the doubly fed induction generator to derive the power losses model in the system by means of the flat outputs and their derivatives. Other applications for system parameters estimation and power losses estimator are detailed in [36].

The flatness-based control improves the system performance and allows implementing a reduced model of the three-phase inverter without loss of dynamical information, when this system is a part of large-scale autonomous or embedded network. A full comparison of flatness control with the conventional control methods like PI and feedback linearization control is done by Houari *et al.*'s work [38]. This comparison shows that the proposed control allows obtaining a low value of voltage THD, high dynamic performances, safety startup, and good robustness against parameter variations.

This paper proposes a new control method based on the flatness control technique for nonisolated power supply which is composed of *N* parallel inverters with an output *LC* filter. The main interest of this control is the possibility to define the behavior of the state variables in the steady state as well as in transient for both dc and ac applications, and the flatness technique is most effective in terms of load sharing and enables reliability and redundancy, although existence of communication between units [29]–[43]. A one-loop flatness-based controller (FBC) is used to set high effective bandwidth to balance the currents between the parallel inverters and to facilitate the reduction of the zero-sequence and circulating current components. The flatness control allows enhancing the behavior of the system under healthy or faulty conditions when one inverter or more of the parallel system are disconnected. Power or current balancing is an important functionality for the parallel power converters or inverters to ensure reliable and efficient operation. One method for controlling parallel inverters is to define an inverter as master which imposes the output voltage while the others are slave and only the currents or power are regulated. The master–slave control has been used in many applications as detailed in [41]–[43]. The proposed control method does not need two control loops, physical or complicated systems, and is independent of the load conditions.

II. Structure Description and Modeling

According to Fig. 1, the sum of the load currents and the sum of the output line currents of all *N* modules are equal to

$$i_{La} + i_{Lb} + i_{Lc} = 0 \tag{1}$$

$$\sum_{k=1}^{N} \left(i_{ak} + i_{bk} + i_{ck} = 0 \right). \tag{2}$$

Then, sum of the capacitive ac bus voltage is constant. The initial value of the capacitor output voltages is zero. Thus, the homopolar voltage component v_{c0} is always zero. Actually, for each inverter of the parallel three-phase inverters system, there is a zero-current path by the antidiodes of the full bridge of the other inverters. To confirm this fact simply, the zero-sequence current of an inverter can be left free and the other $N-1$ zero-sequence currents of the other inverters are kept as independent state variables. Controlling the zero-sequence currents of $N-1$ modules involves the cancellation of the first inverter zero current i_{01}. Then, the homopolar current component of the first inverter can be given as $i_{01} = -\sum_{k=2}^{N} i_{0k}$. The first inverter for the given system is considered as the reference for the given parallel inverters system; it is obvious that another inverter can be considered as the reference or master and the others as slave for the control purposes. In order to establish the control laws in the continuous domain, the voltage–current model is transformed from the three-phase static frame into the synchronous Park frame. Derivatives of the output voltages in *0dq* frame with $v_{c0} = 0$ at the common ac bus are obtained as

$$\begin{pmatrix} \dot{V}_{cd} \\ \dot{V}_{cq} \end{pmatrix} = \begin{pmatrix} 0 & \omega \\ -\omega & 0 \end{pmatrix} \begin{pmatrix} V_{cd} \\ V_{cq} \end{pmatrix} + \frac{1}{C_f} \left(\begin{pmatrix} \sum_{k=1}^{N} i_{dk} \\ \sum_{k=1}^{N} i_{qk} \end{pmatrix} - \begin{pmatrix} i_{Ld} \\ i_{Lq} \end{pmatrix} \right). \tag{3}$$

The derivatives of the *dq* currents of the first inverter as functions of the controlling voltages V_{d1} and V_{q2}, similarly the derivatives of the *K*th currents of the remaining modules with $k \in \{2, \ldots, N\}$, can be obtained as

$$\frac{d}{dt} \begin{pmatrix} i_{d1} \\ i_{q1} \end{pmatrix} = \begin{pmatrix} \frac{-r_1}{L_1} & \omega \\ -\omega & \frac{-r_1}{L_1} \end{pmatrix} \begin{pmatrix} i_{d1} \\ i_{q1} \end{pmatrix} + \frac{1}{L_1} \begin{pmatrix} V_{d1} \\ V_{q1} \end{pmatrix} - \frac{1}{L_1} \begin{pmatrix} V_{cd} \\ V_{cq} \end{pmatrix} \tag{4}$$

$$\frac{d}{dt} \begin{pmatrix} i_{0k} \\ i_{dk} \\ i_{qk} \end{pmatrix} = \begin{pmatrix} \frac{-r_k}{L_k} & 0 & 0 \\ 0 & \frac{-r_k}{L_k} & \omega \\ 0 & -\omega & \frac{-r_k}{L_k} \end{pmatrix} \begin{pmatrix} i_{0k} \\ i_{dk} \\ i_{qk} \end{pmatrix} + \frac{1}{L_k} \begin{pmatrix} V_{0k} \\ V_{dk} \\ V_{qk} \end{pmatrix} - \frac{1}{L_k} \begin{pmatrix} V_{c0} \\ V_{cd} \\ V_{cq} \end{pmatrix} \tag{5}$$

where the variables V_{0k}, V_{dk}, and V_{qk} are the controlling voltages of $(N-1)$th inverters.

III. Parallel Inverter Control Strategy

A one-loop FBC is presented for the control of a system consisting of *N* three-phase parallel inverters. The FBC strategy has been chosen because of its usefulness in situations where

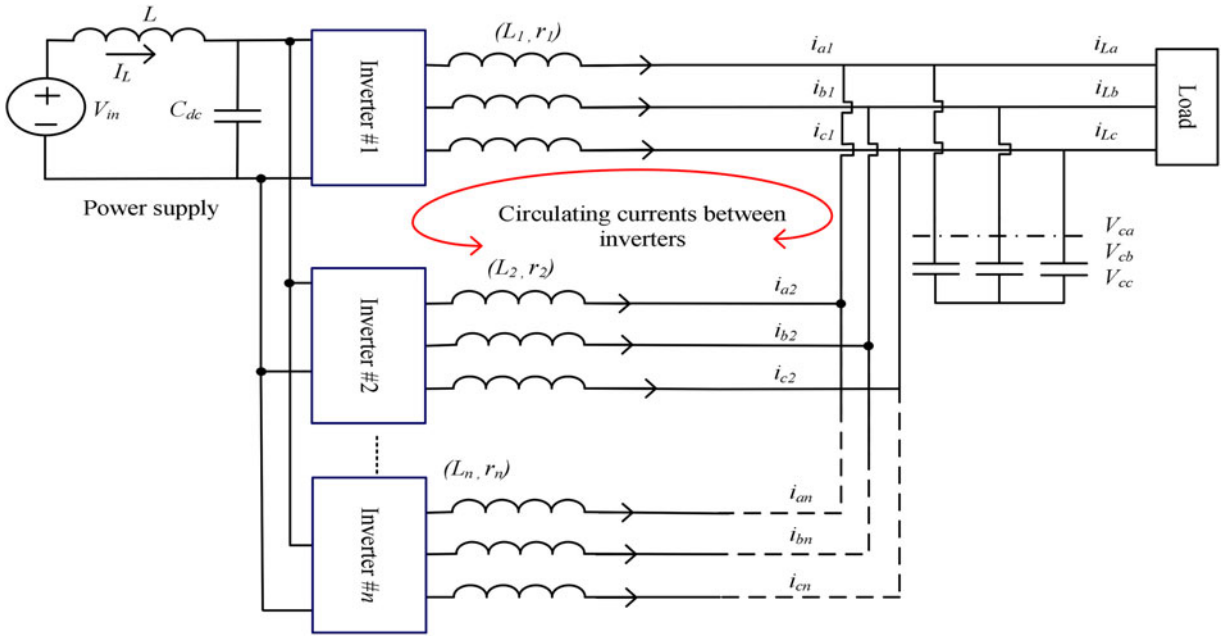

Fig. 1. Architecture of the complete dc-to-ac system of *N* parallel inverters.

explicit trajectories generations are required [29]–[40]. The proposed control strategy ensures the asymptotic stability, high dynamics regulation, and robustness against parameters variations. In fact, the behavior of the system state variables can be planned thanks to given reference trajectories. For the control of differentially flat systems, the major concentration relies on generating feasible trajectories rather than trying to force the system trajectories to converge toward a given operating point. By applying the flatness control, the transient states can be analytically foreseen, which is not always possible with others control strategies. Some properties, applications, and advantages of the FBC systems are detailed in [32]–[40].

A. Introduction to Flatness Control System

The concept of flat systems was introduced by Fliess *et al.* [29] by using the formalism of differential algebra. In the differential algebra, a system is viewed as a differential field by a set of variables (states and inputs). The system is said to be differentially flat if there is a variable called flat output, such that the system is algebraic and nondifferentially over the differential field generated by a set of candidate flat outputs. In fact, a system is flat if an output can be found such that all state variables and input vector components can be determined from this flat output without integration [29]–[32]. More precisely, if the system has a state vector $x \in R^n$ and an input vector $u \in R^m$, then the system is flat if an output $y \in R^m$ can be found in the form given by

$$\begin{cases} y = \phi\left(x, u, \dot{u}, \ldots, u^{(l)}\right) \\ x = \varphi\left(y, \dot{y}, \ldots, y^{(r)}\right) \\ u = \psi\left(y, \dot{y}, \ldots, y^{(r+1)}\right) \end{cases} \tag{6}$$

with rank $(\varphi) = m$, rank $(\varphi) = n$, and rank $(\psi) = m$.

The main interest of application of the flatness is due to some properties which are suitable for the control systems. The main advantages of the flatness control are listed as follows:

1) the flat controllers use the reference signal instead of measured one, this leads to a reduction of the noise impacts (details given in Section III-E);
2) to ensure that the trajectory of the candidate flat output perfectly follows its reference trajectory, I/O feedback linearization technique can be used to avoid the unstable dynamics (no zero dynamic issue when the flatness output is used);
3) the use of reference trajectories of the flat outputs allows ensuring a safe operation during the startup and transients as shown later by simulation and experimental validation;
4) to apply the flatness approach, a candidate flat output which is dependent from the input vector and the state variables has to be found; this is considered as a drawback of the flatness control.

B. Flatness Control of Parallel Inverter System

It is supposed that the variations of the dc bus voltage are compensated by the inverter controller since the voltage V_{dc} is measured. The chosen candidate flat outputs can include any other variables of the system depending on the control purposes. For the control objectives, the electrostatic energy and the current error vector between the parallel inverters are chosen as the candidate flat outputs to regulate the output ac bus voltage and balance the currents between the parallel inverters. So the output voltages will be controlled indirectly by the electrostatic energies. In fact, this choice should lead to a better dynamical behavior regardless of the load perturbations, constant power load systems, or existence of transient state during switching ON/OFF of any inverter for healthy or faulty

operation conditions. The candidate flat outputs vector y is defined as $y = [y_c, y_z]^t$, where the first part $y_c = [y_d, y_q]^t$ is defined by the *dq* electrostatic energies stored in the output capacitive ac bus of the output *LC* filter

$$y_c = \begin{pmatrix} y_d \\ y_q \end{pmatrix} = \frac{1}{2} C_f \begin{pmatrix} \text{sign}(V_{cd}) V_{cd}^2 \\ \text{sign}(V_{cq}) V_{cq}^2 \end{pmatrix} = \phi_{yc}(x). \quad (7)$$

Using y_c given by (7), the system state vector $x = [V_{cd}, V_{cq}]^t$ can be redefined as a function of the flat output vector $y_c = \phi_{yc}(x)$ in form of (6) regarding the sign of the energy vector y_c

$$\begin{pmatrix} V_{cd} \\ V_{cq} \end{pmatrix} = \begin{pmatrix} \text{sign}(y_d)\sqrt{2y_d/C_f} \\ \text{sign}(y_q)\sqrt{2y_q/C_f} \end{pmatrix} = \begin{pmatrix} \varphi_{Vcd}(y_d) \\ \varphi_{Vcq}(y_q) \end{pmatrix}. \quad (8)$$

The second part of the candidate flat output vector y corresponds to the current error vector y_z, which represents the current errors referred to the reference; each component of y_z allows us to minimize the circulating currents and to balance the powers between the reference and all other working kth inverters. The current error vector $y_z = [y_{z1}, y_{z2}, \ldots, y_{zi-1}, y_{zi+1}, \ldots, y_{zN}]^t$ and its components $y_{zk}, \forall k \in \{1, .., N\}, k \neq i$ are expressed as

$$y_{zk} = \begin{pmatrix} y_{zok} \\ y_{zdk} \\ y_{zqk} \end{pmatrix} = \begin{pmatrix} z_{ok} \\ z_{dk} \\ z_{qk} \end{pmatrix} = \begin{pmatrix} i_{0k} \\ i_{di} - i_{dk} \\ i_{qi} - i_{qk} \end{pmatrix} = \phi_{yzk}(x). \quad (9)$$

C. Model of Control for Healthy System

From (3) and (8), the derivatives of the voltage vector $[V_{cd}, V_{cq}]^t$ can be expressed as

$$\begin{pmatrix} \dot{V}_{cd} \\ \dot{V}_{cq} \end{pmatrix} = \begin{pmatrix} 0 & \omega \\ -\omega & 0 \end{pmatrix} \begin{pmatrix} \varphi_{Vcd}(y_d) \\ \varphi_{Vcq}(y_q) \end{pmatrix} + \frac{1}{C_f} \left(\begin{pmatrix} \sum_{j=1}^{N} i_{dj} \\ \sum_{j=1}^{N} i_{qj} \end{pmatrix} - \begin{pmatrix} i_{Ld} \\ i_{Lq} \end{pmatrix} \right). \quad (10)$$

Globally, from (3), (4), and (9), the line currents $[i_{di}, i_{qi}]^t$ of the reference inverter can be expressed as a function of y_c and its derivative $\dot{y}_c$ and y_{zk}

$$\begin{aligned} \begin{pmatrix} i_{di} \\ i_{qi} \end{pmatrix} &= \frac{1}{N} \begin{pmatrix} \text{sign}(y_d)\, \dot{y}_d / \sqrt{2y_d/C_f} + \sum_{\substack{k=1 \\ k \neq i}}^{N} z_{dk} + i_{Ld} \\ \text{sign}(y_q)\, \dot{y}_q / \sqrt{2y_q/C_f} + \sum_{\substack{k=1 \\ k \neq i}}^{N} z_{qk} + i_{Lq} \end{pmatrix} \\ &\quad - \begin{pmatrix} 0 & \frac{\omega C_f}{N} \\ -\frac{\omega C_f}{N} & 0 \end{pmatrix} \begin{pmatrix} \text{sign}(y_d)\sqrt{2y_d/C_f} \\ \text{sign}(y_q)\sqrt{2y_q/C_f} \end{pmatrix} \\ &= \begin{pmatrix} \varphi_{i_{di}}(y_c, \dot{y}_c, y_z) \\ \varphi_{i_{qi}}(y_c, \dot{y}_c, y_z) \end{pmatrix}. \end{aligned} \quad (11)$$

The expression $i_{0dqk} (k \in \{(1, .., N\}, k \neq i)$ for the line currents of the remaining inverters can be derived using (9) and substituting from (11)

$$\begin{pmatrix} i_{0k} \\ i_{dk} \\ i_{qk} \end{pmatrix} = \begin{pmatrix} z_{0k} \\ \varphi_{i_{di}}(y_c, \dot{y}_c, y_z) - z_{dk} \\ \varphi_{i_{qi}}(y_c, \dot{y}_c, y_z) - z_{qk} \end{pmatrix} = \begin{pmatrix} \varphi_{i_{0k}}(y_{zk}) \\ \varphi_{i_{dk}}(y_c, \dot{y}_c, y_{zk}) \\ \varphi_{i_{qk}}(y_c, \dot{y}_c, y_{zk}) \end{pmatrix}. \quad (12)$$

The current derivatives of the reference inverter by using (10) and (11) can be obtained as (13) as shown at the bottom of the page.

The derivatives of the remaining line currents i_{0dqk} $\forall k \in \{1, .., N\}, k \neq i$ verify

$$\begin{aligned} \frac{d}{dt} \begin{pmatrix} i_{0k} \\ i_{dk} \\ i_{qk} \end{pmatrix} &= \begin{pmatrix} \dot{z}_{0k} \\ \varphi_{di_{di}}(y_c, \dot{y}_c, \ddot{y}_c, y_z, \dot{y}_z) - \dot{z}_{dk} \\ \varphi_{di_{qi}}(y_c, \dot{y}_c, \ddot{y}_c, y_z, \dot{y}_z) - \dot{z}_{qk} \end{pmatrix} \\ &= \begin{pmatrix} \varphi_{di_{0k}}(\dot{y}_z) \\ \varphi_{di_{dk}}(y_c, \dot{y}_c, \ddot{y}_c, y_z, \dot{y}_z) \\ \varphi_{di_{qk}}(y_c, \dot{y}_c, \ddot{y}_c, y_z, \dot{y}_z) \end{pmatrix}. \end{aligned} \quad (14)$$

$$\begin{aligned} \frac{d}{dt} \begin{pmatrix} i_{di} \\ i_{qi} \end{pmatrix} &= \frac{1}{N} \left(\begin{pmatrix} \frac{\text{sign}(y_d)\, \ddot{y}_d}{V_{cd}} - \frac{\text{sign}(y_d)\, \dot{y}_d}{C_f V_{cd}^2} \left(\sum_{j=1}^{N} i_{dj} - i_{Ld} + \omega C_f V_{cq} \right) \\ \frac{\text{sign}(y_q)\, \ddot{y}_q}{V_{cq}} - \frac{\text{sign}(y_q)\, \dot{y}_q}{C_f V_{cq}^2} \left(\sum_{j=1}^{N} i_{qj} - i_{Lq} - \omega C_f V_{cd} \right) \end{pmatrix} \right. \\ &\quad \left. + \begin{pmatrix} \sum_{\substack{k=1 \\ k \neq i}}^{N} \dot{z}_{dk} + \frac{d}{dt} i_{Ld} \\ \sum_{\substack{k=1 \\ k \neq i}}^{N} \dot{z}_{qk} + \frac{d}{dt} i_{Lq} \end{pmatrix} - \begin{pmatrix} 0 & \omega \\ -\omega & 0 \end{pmatrix} \left(\begin{pmatrix} \sum_{j=1}^{N} i_{dj} - i_{Ld} + \omega C_f V_{cq} \\ \sum_{j=1}^{N} i_{qj} - i_{Lq} - \omega C_f V_{cd} \end{pmatrix} \right) \right) \\ &= \begin{pmatrix} \varphi_{di_{di}}(y_c, \dot{y}_c, \ddot{y}_c, y_z, \dot{y}_z) \\ \varphi_{di_{qi}}(y_c, \dot{y}_c, \ddot{y}_c, y_z, \dot{y}_z) \end{pmatrix} \end{aligned} \quad (13)$$

From (11)–(14), the line currents and their respective derivatives are found as a function of the candidate flat output as given by (6). Globally, the input controlling vector $u = [V_{di}, V_{qi}, \ldots V_{0k}, V_{dk}, V_{qk}]^t$ can be obtained as

$$\begin{pmatrix} V_{di} \\ V_{qi} \end{pmatrix} = L_1 \begin{pmatrix} \varphi_{di_{di}} \\ \varphi_{di_{qi}} \end{pmatrix} - L_i \begin{pmatrix} \frac{-r_i}{L_i} & \omega \\ -\omega & \frac{-r_i}{L_i} \end{pmatrix} \begin{pmatrix} \varphi_{i_{di}} \\ \varphi_{i_{qi}} \end{pmatrix} + \begin{pmatrix} \varphi_{V_{cd}} \\ \varphi_{V_{cq}} \end{pmatrix} = \begin{pmatrix} \psi_{V_{di}}\left(y_c, \dot{y}_c, \ddot{y}_c, y_{zk}, \dot{y}_{zk}\right) \\ \psi_{V_{qi}}\left(y_c, \dot{y}_c, \ddot{y}_c, y_{zk}, \dot{y}_{zk}\right) \end{pmatrix}. \quad (15)$$

By the same analysis, the input control vector of the $N-1$ remaining inverters $\forall k \in \{1, .., N\}, k \neq i$ can be obtained as

$$\begin{pmatrix} V_{0k} \\ V_{dk} \\ V_{qk} \end{pmatrix} = L_k \begin{pmatrix} \varphi_{di_{0k}} \\ \varphi_{di_{dk}} \\ \varphi_{di_{qk}} \end{pmatrix} - L_k \begin{pmatrix} \frac{-r_k}{L_k} & 0 & 0 \\ 0 & \frac{-r_k}{L_k} & \omega \\ 0 & -\omega & \frac{-r_k}{L_k} \end{pmatrix} \times \begin{pmatrix} \varphi_{i_{0k}} \\ \varphi_{i_{dk}} \\ \varphi_{i_{qk}} \end{pmatrix} + \begin{pmatrix} V_{c0} \\ \varphi_{V_{cd}} \\ \varphi_{V_{cq}} \end{pmatrix} = \begin{pmatrix} \psi_{V_{0k}}\left(y_z, \dot{y}_z\right) \\ \psi_{V_{dK}}\left(y_c, \dot{y}_c, \ddot{y}_c, y_z, \dot{y}_z\right) \\ \psi_{V_{qK}}\left(y_c, \dot{y}_c, \ddot{y}_c, y_z, \dot{y}_z\right) \end{pmatrix}. \quad (16)$$

D. Model of Control for Faulty System Conditions

If one inverter (including the reference one) or more of the parallel system are disconnected under normal or faulty conditions, the previous analysis is always valid and the rank of the states vector x will be reduced by $3f$, where f is the number of the faulty inverters (i.e., $x \in R^{n-3f}$). The ranks of the flat output vector y and the input u will also be reduced by $3f$, but the y_c rank rests the same (i.e., $y \in R^{m-3f}$). When the reference inverter (the first one by example) is fully disconnected, the current expression given by (11) will be referred to the next inverter by example the second one. Consequently, (9) will be referred to the new reference. The flatness conditions can always be verified for the studied system with the reduced state and input vectors associated with the candidate flat output y regarding the new vector y_{zk}. The reference y_{zk_ref} of the current error vector y_{zk} is assumed to be zero in normal case (i.e., $z_{ok\_\mathrm{ref}} = z_{dk\_\mathrm{ref}} = z_{qk\_\mathrm{ref}} = 0$). This choice minimizes the circulating currents and ensures that the load power is equally shared between the parallel inverters.

When one inverter (number j for example) of the parallel system is fully disconnected, the reference y_{zj_ref} of the current error vector y_{zj} becomes equal to the reference inverter currents (i.e., $z_{oj\_\mathrm{ref}} = 0, z_{dj\_\mathrm{ref}} = i_{di}, z_{qj\_\mathrm{ref}} = i_{qi}$). Thus, in the case of the healthy or faulty conditions of any inverter in the parallel system, the relations (11) and (13) can always be used. For both cases, the references of y_c are calculated as

$$y_{c\_\mathrm{ref}} = \begin{pmatrix} y_{d\_\mathrm{ref}} \\ y_{q\_\mathrm{ref}} \end{pmatrix} = \frac{1}{2} C_f \begin{pmatrix} V^2_{cd_{\mathrm{ref}}} \\ V^2_{cq_{\mathrm{ref}}} \end{pmatrix} \quad (17)$$

where $V_{cd_{\mathrm{ref}}} = V_{cq_{\mathrm{ref}}} = V_{\mathrm{rms}}\sqrt{3/2}$ and V_{rms} represents the RMS value of the voltage reference of the output ac bus instead of using the instantaneous value to avoid using the time dependent component, where the references y_{zk_ref} are forced to be null for the healthy conditions to minimize the circulating currents (i.e., $z_{ok\_\mathrm{ref}} = z_{dk\_\mathrm{ref}} = z_{qk\_\mathrm{ref}} = 0$), where the load power is equally shared between the parallel inverters. But under normally or faulty disconnection of any inverter, its respective currents i_{df_i} and i_{qf_i} are zero where $f_i \in \{N\}$ is the identification number of the faulty inverter; then, both concerning flat output components $z_{dfi\_\mathrm{ref}}, z_{qfi\_\mathrm{ref}}$ between this disconnected inverter and the reference and their respective derivatives are no more zero. The last step consists in the formulation of the input vector u as a function of the candidate flat output reference $y_{\_\mathrm{ref}} = [y_{c\_\mathrm{ref}}, y_{z\_\mathrm{ref}}]^t$ and their respective derivatives. The relations (15) and (16) can be expressed for each active inverter as

$$\begin{pmatrix} V_{di} \\ V_{qi} \end{pmatrix} = \begin{pmatrix} \psi_{V_{di}}\left(y_{c\_\mathrm{ref}}, \dot{y}_{c\_\mathrm{ref}}, \ddot{y}_{c\_\mathrm{ref}}, y_{z\_\mathrm{ref}}, \dot{y}_{z\_\mathrm{ref}}\right) \\ \psi_{V_{qi}}\left(y_{c\_\mathrm{ref}}, \dot{y}_{c\_\mathrm{ref}}, \ddot{y}_{c\_\mathrm{ref}}, y_{z\_\mathrm{ref}}, \dot{y}_{z\_\mathrm{ref}}\right) \end{pmatrix} \quad (18)$$

$$\begin{pmatrix} V_{0k} \\ V_{dk} \\ V_{qk} \end{pmatrix} = \begin{pmatrix} \psi_{V_{0k}}\left(y_{z\_\mathrm{ref}}, \dot{y}_{z\_\mathrm{ref}}\right) \\ \psi_{V_{dK}}\left(y_{c\_\mathrm{ref}}, \dot{y}_{c\_\mathrm{ref}}, \ddot{y}_{c\_\mathrm{ref}}, y_{z\_\mathrm{ref}}, \dot{y}_{z\_\mathrm{ref}}\right) \\ \psi_{V_{qK}}\left(y_{c\_\mathrm{ref}}, \dot{y}_{c\_\mathrm{ref}}, \ddot{y}_{c\_\mathrm{ref}}, y_{z\_\mathrm{ref}}, \dot{y}_{z\_\mathrm{ref}}\right) \end{pmatrix}. \quad (19)$$

The dynamic behavior of the input dc bus voltage and input current can be investigated thanks to the following differential equations:

$$V_{in} = L\frac{di_L}{dt} + r_L i_L + V_{DC} \quad (20)$$

$$C_{dc}\frac{dV_{dc}}{dt} = i_L - \frac{1}{V_{dc}}\sum_{k=1}^{N}\left(V_{dk}i_{dk} + V_{qk}i_{qk}\right). \quad (21)$$

E. Reference Trajectory Definition

To plan the desired trajectory of the candidate flat output y and consequently their subrespective components as given by (7) and (9), a low-pass second-order filter is used, which allows limiting the power during transient state due to variations of the voltage reference value V_{rms}. At the input of these filters are connected the reference y_{c_ref} and y_{zk_ref} discussed in Section III-D. Moreover, such formulation allows respecting the conditions of the candidate flat output derivatives at the initial time and in the steady state. At these instants, the values of these derivatives have to be zero. Therefore, the desired reference trajectory $y_{\mathrm{ref}} = [y_{c_{\mathrm{ref}}}, y_{z_{\mathrm{ref}}}]^t$ $\forall k \in \{1, .., N\}, k \neq i$ can be expressed as

$$y_{c\mathrm{ref}} = \left(1 - \left(1 + \frac{t - t_{\mathrm{init}c}}{\tau_{1c}}\right)e^{-\frac{t-t_{\mathrm{init}c}}{\tau_{1c}}}\right) \times \left(y_{c_{\mathrm{ref}}} - y_{c_{\mathrm{init}}}\right) + y_{c\_\mathrm{init}} \quad (22)$$

$$y_{zk\mathrm{ref}} = \left(1 - \left(1 + \frac{t - t_{\mathrm{init}c}}{\tau_{1c}}\right)e^{-\frac{t-t_{\mathrm{init}z}}{\tau_{2z}}}\right) \times \left(y_{zk_{\mathrm{ref}}} - y_{zk_{\mathrm{init}}}\right) + y_{zk\_\mathrm{init}} \quad (23)$$

TABLE I
SYSTEM PARAMETERS

DC side line inductances	$L = 400\ \mu$H, $r_L = 0.2\ \Omega$
Output ac filter inductances	$L_1 = L_2 = L_3 = 1$ mH, $r_1 = r_2 = r_3 = 0.7\ \Omega$
DC bus capacitance	$C_{dc} = 1100\ \mu$F
Output filter capacitance	$C_f = 40\ \mu$F
AC output voltages	110 V–60 Hz
DC input voltages	500 V
Switching frequency	$f_{\rm sw} = 15$ kHz
Energy trajectory dynamics	$\xi_c = 0.7, \omega_{yc} = 5000$ rad/s, $p_1 = 6000$ rad/s
Current trajectory dynamics	$\xi_z = 0.7, \omega_{yz} = 5000$ rad/s,
Time constant (τ_{1c})	10 ms
Time constant (τ_{2c})	1 ms

where t and $t_{\text{init}c/z}$ represent the time and the initial time for both reference trajectories, respectively, and τ_{1c} and τ_{2z} are the time constants of the planed reference trajectories for the electrostatic energy and the current error. The design of the time constant τ_{1c} (the same procedures for τ_{2z}) is realized in [32] to respect the power supply constraints; the constants values are given in Table I.

F. Control Law and Linearization

To ensure the control of both trajectories of the energy y_c and the current error y_{zk} to their respective reference trajectories $y_{c\text{ref}}$ and $y_{zk\text{ref}}$ for the healthy or faulty conditions, a classical input–output linearization is used. Feedback linearization is a common approach used in the control of the nonlinear systems. This approach can be done by obtaining a linear input–output behavior of a modified system. This involves transformation of the nonlinear system into an equivalent algebraic linear system through changing the control variables and inputs. Feedback linearization can be applied to the nonlinear parallel inverters system discussed in this paper. The main disadvantage of feedback linearization is its weakness in the presence of parameter uncertainties. This technique consists in introducing fictitious control variables $\gamma_c = [\gamma_d, \gamma_q]^t$ associated with the output energy vector and $[\gamma_z = \gamma_{z1}, .., \gamma_{zi-1}, \gamma_{zi+1}, .., \gamma_{zN}]^t$ for the current error vector. For the output energy vector, it can be expressed in the form of the fictitious control variables γ_c as

$$\begin{cases} \ddot{y}_d = \gamma_d \\ \ddot{y}_q = \gamma_q. \end{cases} \tag{24}$$

These controls laws allow an asymptotic convergence of the measured variables to their respective reference trajectories and can be deduced as

$$\begin{aligned} &(\ddot{y}_{d_{\text{ref}}} - \gamma_d) + k_{11}\,(\dot{y}_{d_{\text{ref}}} - \dot{y}_d) + k_{12}\,(y_{d_{\text{ref}}} - y_d) \\ &\quad + k_{13}\int (y_{d\text{ref}} - y_d)\,d\tau = 0 \end{aligned} \tag{25}$$

$$\begin{aligned} &(\ddot{y}_{q_{\text{ref}}} - \gamma_q) + k_{11}\,(\dot{y}_{q_{\text{ref}}} - \dot{y}_q) + k_{12}\,(y_{q_{\text{ref}}} - y_q) \\ &\quad + k_{13}\int (y_{q\text{ref}} - y_q)\,d\tau = 0. \end{aligned} \tag{26}$$

The integral term is introduced to ensure zero static error in steady state and compensate the effects introduced by the system modeling errors. For each current error vector y_{zk}, the fictitious control variable $\gamma_{zk} = [\gamma_{z0k}, \gamma_{zdk}, \gamma_{zqk}]^t$ is introduced and expressed in the same way for the output energy vector as

$$\gamma_{zk} = \begin{cases} \dot{z}_{0k} = \gamma_{z0k} \\ \dot{z}_{dk} = \gamma_{zdk} \\ \dot{z}_{qk} = \gamma_{zqk} \end{cases} \quad \forall k \in \{1, \ldots, N\}, k \neq i. \tag{27}$$

Second-order laws are used to ensure that the current error vector y_{zk} follows its planed reference $y_{zk\text{ref}}$:

$$\begin{aligned} &(\dot{y}_{zk_{\text{ref}}} - \gamma_{zk}) + k_{21}\,(y_{zk_{\text{ref}}} - y_{zk}) \\ &\quad + k_{22}\int (y_{zk\text{ref}} - y_{zk})\,d\tau = 0. \end{aligned} \tag{28}$$

To simplify (25), (26), and (28), a variable ε is introduced to express dynamics of the error

$$\dddot{\varepsilon}_{y_c} + k_{11}\ddot{\varepsilon}_{y_c} + k_{12}\dot{\varepsilon}_{y_c} + k_{13}\varepsilon_{y_c} = 0 \tag{29}$$

$$\ddot{\varepsilon}_{y_z} + k_{21}\dot{\varepsilon}_{y_z} + k_{22}\varepsilon_{y_z} = 0 \tag{30}$$

where $\varepsilon_{y_c} = y_{c\text{ref}} - y_c$ and $\varepsilon_{y_{zk}} = y_{zk\text{ref}} - y_{zk}$.

The parallel system operating point will be stable if the coefficients $k_{11}, k_{12}, k_{13}, k_{21}, k_{22}$ are strictly positive values. The dynamics of the system will be fixed by these gains associated with the control laws; their values are given in Table I. To determine values of the gain coefficients, a classical pole placement method is used thanks to a comparison between the characteristic polynomials associated with (29) and (30) with the polynomials (31); therefore, the control gains parameters can be defined

$$\begin{cases} p_{yc}\,(s) = (s + p_1)\left(s^2 + 2.\xi.\omega_n.s + \omega_n^2\right) \\ p_{yz}\,(s) = \left(s^2 + 2.\xi.\omega_n.s + \omega_n^2\right) \end{cases} \tag{31}$$

$$\begin{cases} k_{11} = 2.\xi_c.\omega_{y_c} + p_1 \\ k_{12} = 2.\xi_c.\omega_{y_c}.p_1 + \omega_{y_c}^2 \\ k_{13} = p_{y_c}.\omega_{y_c}^2 \end{cases} \tag{32}$$

$$\begin{cases} k_{21} = 2.\xi_z.\omega_{y_z} \\ k_{22} = \omega_{y_z}^2\,. \end{cases} \tag{33}$$

It is possible to get the formulation of u in closed loop by

$$\begin{pmatrix} V_{di} \\ V_{qi} \end{pmatrix} = \begin{pmatrix} \psi_{V_{d1}}\,(y_{c\text{ref}}, \dot{y}_{c\text{ref}}, \gamma_c, y_{z\text{ref}}, \gamma_z) \\ \psi_{V_{q1}}\,(y_{c\text{ref}}, \dot{y}_{c\text{ref}}, \gamma_c, y_{z\text{ref}}, \gamma_z) \end{pmatrix} \tag{34}$$

$$\begin{pmatrix} V_{0k} \\ V_{dk} \\ V_{qk} \end{pmatrix} = \begin{pmatrix} \psi_{V_{0k}}\,(y_{zk\text{ref}}, \gamma_z) \\ \psi_{V_{dK}}\,(y_{c\text{ref}}, \dot{y}_{c\text{ref}}, \gamma_c, y_{z\text{ref}}, \gamma_z) \\ \psi_{V_{qK}}\,(y_{c\text{ref}}, \dot{y}_{c\text{ref}}, \gamma_c, y_{z\text{ref}}, \gamma_z) \end{pmatrix}. \tag{35}$$

IV. SIMULATION RESULTS

To validate the proposed control method, a model based on MATLAB-Simulink has been performed; three parallel inverters system are considered (i.e., $N = 3$). The system parameters and the control gains which are associated with the energy and current balancing trajectories are identical to those used for the

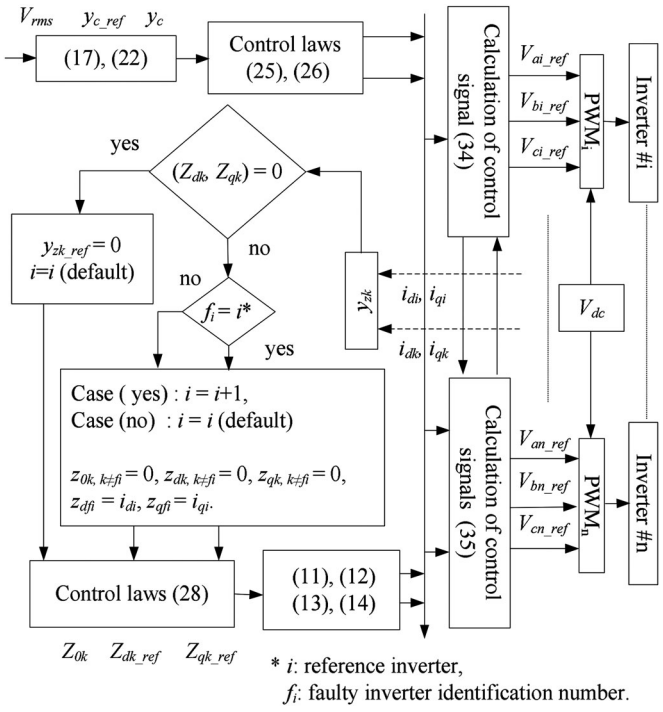

Fig. 2. Operational diagram of the proposed control method for N-parallel inverters with the circulating current and balancing method.

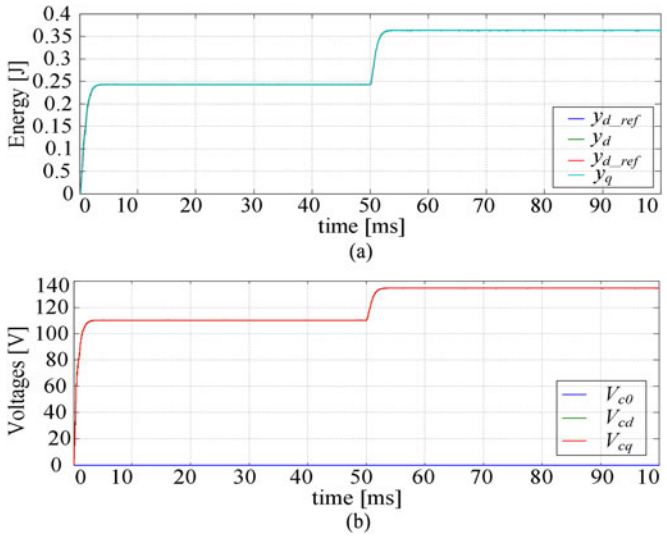

Fig. 3. Waveforms of output ac bus of parallel system under the proposed control method. (a) Behavior of electrostatic energies y_d and y_q. (b) Voltages V_{c0}, V_{cd}, and V_{cq} of output ac bus from startup to a step of output voltage $V_{\rm rms}$ at $t = 50$ ms from 90 to 110 V.

experimental validations as listed in Table I. The schematic diagram of the proposed control system is given in Fig. 2. Under the normal conditions, the proposed control method regulates the output ac bus voltages. The current balancing controller shares the load power between the parallel inverters with minimization of the circulating currents, so the current error vector y_{zk} equals zero. Under the abnormal conditions of any inverter, the corresponding current error vector y_{zk} referred to the reference inverter is no more zero. This method can be used for multiple inverters failure identification, if the value of the individual current error vector y_{zk} equals the reference inverter dq currents; this value will be an indication for the full disconnection of the faulty inverter. So the proposed control given by (9) and (28) is verified for both healthy and faulty conditions. Fig. 3(a) and (b) shows, respectively, the behavior of the electrostatic energies y_d and y_q and the corresponding output voltages V_{cd} and V_{cq} under normal conditions for a step of the RMS reference value from 90 to 110 V at $t = 50$ ms. The measured components follow perfectly their respective reference trajectories with the time constant (τ_{1c}) listed in Table I. The components y_0 and V_{c0} equal zero. In this case, when the three modules are identical, there is no circulating current.

Fig. 4(a) shows the behavior of the line currents i_{a1}, i_{a2}, and i_{a3} and the corresponding powers P_1, P_2, and P_3 between the three inverters at the PCC during abnormal conditions, by adding 1.5 Ω per phase for the second inverter with and without the current balancing method for the values of $V_{dc} = 500$ V, $V_{\rm rms} = 110$ V, and the load power of 3.2 kW. When the current balancing controller is switched OFF at $t = 40$ ms, the healthy inverters carry more power than the faulty. So, there is a circulating current between the parallel. Fig. 4(b) shows the power sharing between the three inverters; the three powers are supposed to be equal as indicated by the normal zone ZN. The load power P_L is divided equally to P_1, P_2, and P_3 at the PCC between the three inverters for a given load of 3.2 kW. If a fault involves full disconnection of one inverter by example in the second inverter at $t = 20$ ms, the reference inverter and the third continue equally supplying the load during the abnormal zone ZF2. When the second inverter problem was cleared at $t = 40$ ms, the load power is equally shared as before in ZN. The same operation can be applied for the third inverter when the disconnection and reclosure are occurred at $t = 60$ ms and $t = 80$ ms, respectively, in ZF3. In the zones ZF2 and ZF3, the first inverter is the reference as viewed by the current error vector y_{zk}, but if it is disconnected, the currents will be referred to the second inverter as given by (9) and operational diagram as shown in Fig. 2 (i.e., $i = 2$).

Fig. 4(c) shows the current error behavior during the healthy and abnormal conditions; the current error vector equals zero for ZN, and when the second inverter is fully disconnected, the current error vector equals the current of the reference inverter. Fig. 4(d) shows the behavior of the electrostatic energies when the second inverter or the third is disconnected. Some perturbations about 6% of the steady-state value are observed at both $t = 20$ ms and $t = 60$ ms; this is due to the variations of the electromagnetic energy stored in the line inductances which influence the ac bus energy. When the faults are cleared and the inverter is reconnected to the PCC, the perturbations are negligible as indicated at $t = 40$ ms and $t = 80$ ms. The current balancing controller limits the rate of variations of the reference trajectories at the reclosure moment after clearing the problems of disconnected inverter. The behavior of the voltage V_{cd}, V_{cq} and three-phase voltages V_{ca}, V_{cb}, and V_{cc} of the output ac bus is shown in Fig. 4(e) when one inverter is disconnected. Some

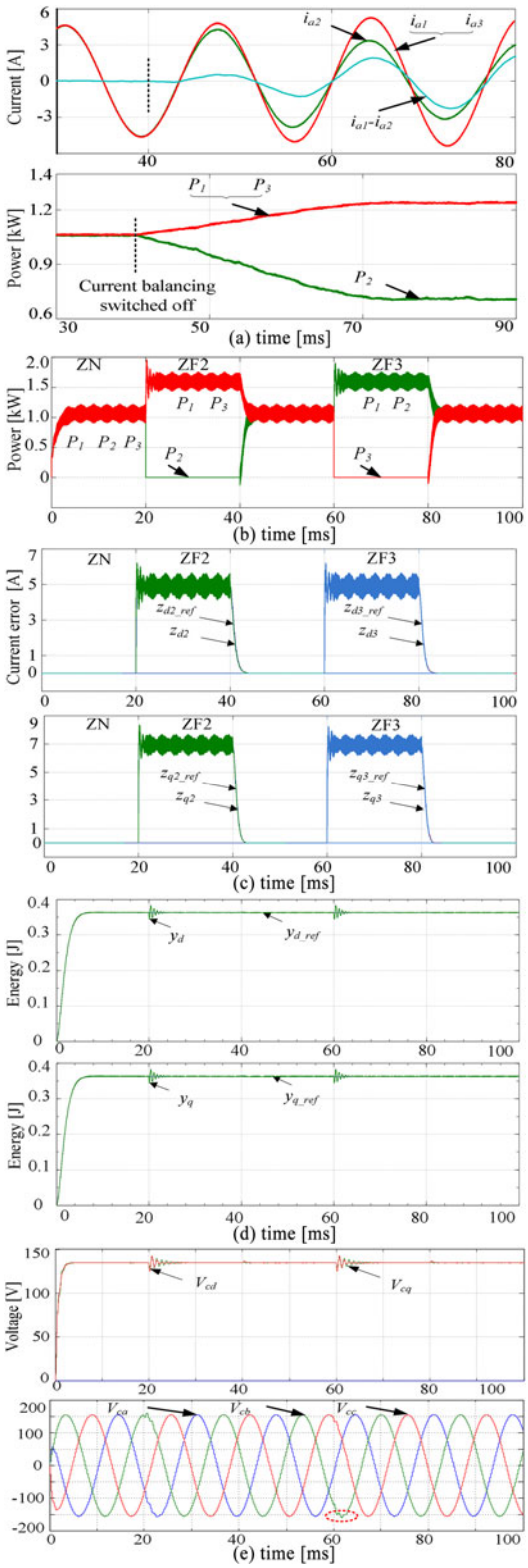

Fig. 4. Behavior of parallel system under the proposed control method ($V_{dc} = 500$ V, $V_{\rm rms} = 110$ V, $P_{\rm load} = 3.2$ kW). (a) Line currents and power sharing between parallel inverters for a load of 3.2 kW when the current balancing controller is switched OFF. (b) Load power sharing between parallel inverters for a load of 3.2 kW during healthy and faulty operation conditions for each inverter with the proposed current balancing method. (c) Behavior of current error during healthy and faulty conditions. (d) Behavior of electrostatic energies y_d, y_q under the proposed current balancing method with minimal perturbation. (e) Behavior of V_{cd}, V_{cq} and output three-phase voltages.

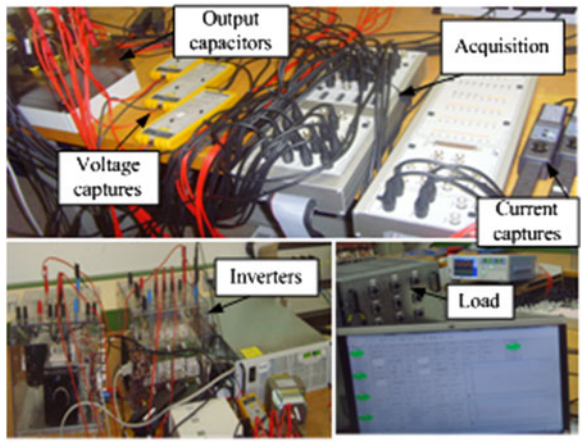

Fig. 5. Experimental bench of two parallel inverter system.

perturbations about 6% of the steady-state value are observed at the moment of full disconnection of the second inverter or the third. Elsewhere the perturbations, the output energies and capacitive bus voltages follow perfectly their respective reference trajectories and the three-phase voltages of the output ac bus are pure sine waves.

V. Experimental Results

To verify the validity of the proposed control method, experiments are performed on a 5-kW workbench consisting of two parallel inverters under the proposed control method and the photographs as shown in Fig. 5 with the parameters listed in Table I. The control is realized with MATLAB-Simulink-RTW software and implemented owing to dSPACE-1105 real-time control card. Fig. 6(a) shows the output ac bus voltages for a balanced resistive load of 3.2 kW. The reported voltage THD is 1.8% for the FBC. Fig. 6(b) shows the behavior of both the *dq* energies and voltages of the output ac bus after a step variation of the voltage reference from 55 to 110 V with a resistive load power set to 3.2 kW in steady state. The measured values follow perfectly their respective reference trajectories. Fig. 6(c) shows the experimental results of the output energies which follow perfectly the planed energy references for a step variations from 120 to 80 V and then again to 120 V. The behavior of the output energy stays well controlled thanks to the proposed flat control method after a step of the load power from 3.2 to 5 kW. The system exhibits efficiency about 87% under the given load conditions. When there is no similarity of the components, there will be a circulating currents between the parallel inverters, unbalanced conditions are introduced by adding 1.5 Ω per phase for the second inverter, this resistance artificially represents the nonequilibrating conditions, the currents i_{d1}, i_{d2} and i_{q1}, i_{q2} at the PCC are still equally divided between the two inverters by the current balancing controller, and the circulating current is reduced to zero as shown in Fig. 6(d) and (e). The current respective differences are equal to zero with the proposed currents balancing method. These results put emphasis on minimization of the circulating currents for unbalanced

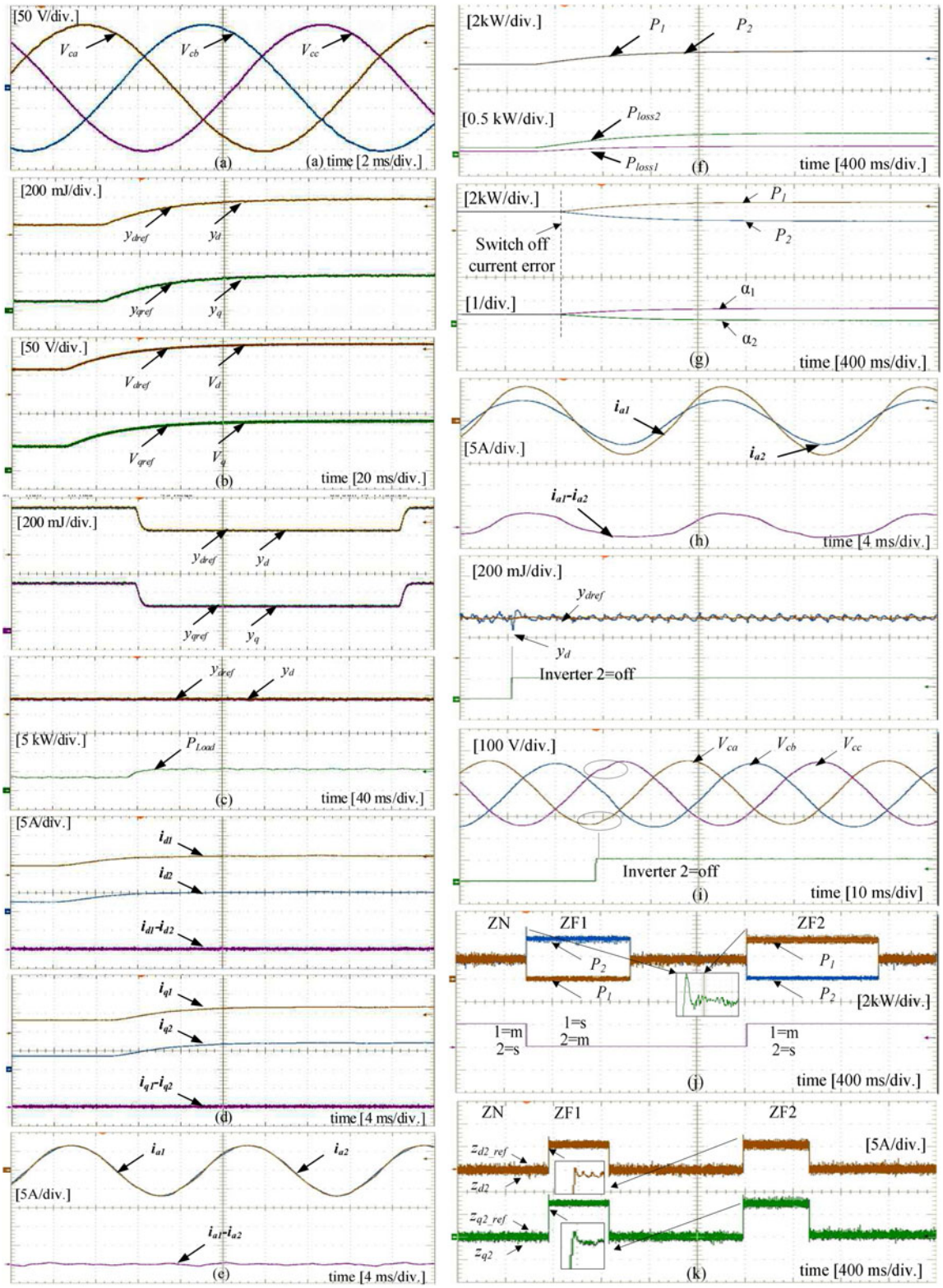

Fig. 6. Experimental waveforms of the proposed control method ($V_{dc} = 500$ V, $V_{\rm rms} = 110$ V, $P_{\rm load} = 3.2$ kW). (a) Output ac bus voltages for $V_{\rm rms}$ 110 V under 3.2-kW balanced resistive load. (b) Behavior of measured *dq* energies and output voltages for step of $V_{\rm rms}$ from 55 to 110 V. (c) Energies after step variation of $V_{\rm rms}$ from 120 to 80 V and then again to 120 V and with step of load power from 3.2 to 5 kW. (d) Currents i_{d1}, i_{d2} and i_{q1}, i_{q2} and their respective differences when current balancing controller in on state. (e) Line currents i_{a1}, i_{a2} and their respective differences when current balancing controller in on state. (f) Corresponding behavior of supplied power P_1, P_2 losses $P_{\rm loss1}$ and $P_{\rm loss2}$ at PCC. (g) Power P_1, P_2 and their ratio at PCC under resistive balanced load of 3.2 kW when current balancing controller is in off state. (h) Line currents i_{a1}, i_{a2} and their respective differences when current balancing controller is in off state. (i) Behavior of electrostatic energies y_d and y_q during full disconnection of second inverter and corresponding three-phase voltages with perturbation of 7%. (j) Power P_1 and P_2 at PCC under resistive balanced load of 3.2 kW for full disconnection of first and second inverters, respectively. (k) Current error vector z_{d2} and z_{q2} components and their reference trajectories under resistive balanced load of 3.2 kW for full disconnection condition of parallel inverters.

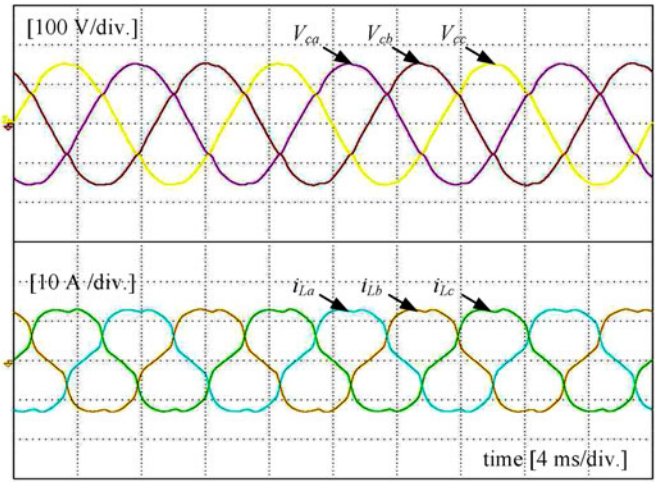

Fig. 7. Experimental results for output ac bus voltages and load currents with a nonlinear load ($V_{dc} = 500$ V, $V_{\rm rms} = 110$ V, $P_{\rm load} = 3.2$ kW).

parallel systems. Fig. 6(f) shows the power P_1, P_2 which are balanced between the two parallel inverters, but the second inverter exhibits more losses than the first under the given nonequilibrating conditions. These figures show the efficiency of the current balancing method which has to be used to balance the currents and powers between the parallel inverters. The current balancing controller is still efficient during the transient state.

Fig. 6(g) shows the power P_1, P_2 and the power sharing ratio α_1, α_2 between the two inverters under a resistive balanced load of 3.2 kW when the current balancing controller is switched OFF under the abnormal conditions by adding 1.5 Ω per phase for the second inverter. The healthy inverter provides more power than the faulty. So, there is a circulating current about 2 A between the parallel inverters as shown in Fig. 6(h). The system exhibits efficiency about 86% and 84% with and without the current balancing method under the abnormal conditions and the same load conditions. Fig. 6(i) shows the behavior of electrostatic energies y_d (similarly y_q) and the output ac bus voltages $V_{\rm abc}$ during the faulty conditions of the second inverter which is fully disconnected for the given values of $V_{dc} = 500$ V, $V_{\rm rms} = 110$ V and the load power of 3.2 kW. Perturbation around 7% in comparison with the steady-state value is observed for the energy and output ac bus voltages due to change of the electromagnetic energy level in the line inductors. The corresponding behavior of the power P_1, P_2 and current error z_d, z_q and their respective reference trajectories is shown in Fig. 6(j) and (k); when the first inverter is fully switched OFF at the beginning of ZF1, the full load power is provided by the second inverter which becomes the reference (i.e., inv1 = s, inv2 = m) and continues as the reference. However, at the reclosure of the first inverter at the end of ZF1, the second inverter stays the reference until it is disconnected at the beginning of ZF2, and the first inverter becomes the reference as in the initial state. To verify the performance of the proposed control method under nonlinear load conditions, three-phase diode bridge rectifier with a resistive load is used. Fig. 7 shows the waveforms of the output ac bus voltages and load currents; the THD is 2.71% for the output ac bus voltages and 12.33% for the load currents under the

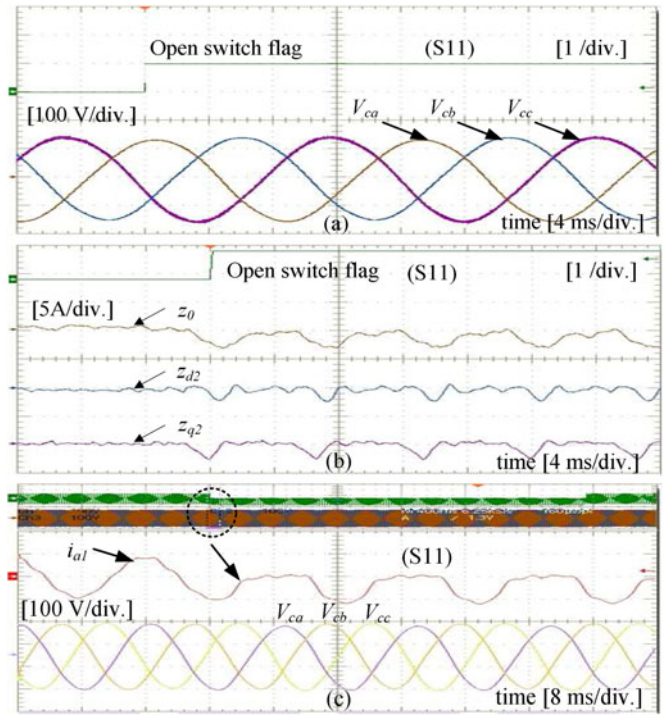

Fig. 8. Experimental waveforms of output ac bus voltages and line currents under open-switch fault ($V_{dc} = 500$ V, $V_{\rm rms} = 110$ V, $P_{\rm load} = 3.2$ kW). (a) Output ac bus voltages under open-switch fault. (b) Corresponding current error for open-switch fault. (c) Line current i_{a1} and output ac bus voltages under open-switch fault.

proposed control method. The low-voltage THD value under the flatness controller is mainly due to use of the reference trajectories reactions instead of disturbance reactions. The performance of the proposed control method can be tested under abnormal conditions like open-switch fault. Fig. 8(a) shows the experimental results for the output ac bus voltages under open-switch fault for S11 as upper switch of the first inverter with a detection variable flag.

In this case, the control continues to operate in normal mode (no disconnection of the faulty inverter). The measured current error values are negative for the upper open-switch case as shown in Fig. 8(b). The faulty phase has negative unidirectional current and zero for the positive half as shown in Fig. 8(c). The experimental results show the validity of the proposed FBC method for regulating the output ac bus voltage and minimizing the circulating currents between the parallel inverters and minimizing the transient effects due to changes of the parallel inverters configuration. This FBC control method can be extended to other parallel dc-to-dc or dc-to-ac systems.

VI. Conclusion

This paper has presented a parallel system consists of *N* three-phase inverters with an output *LC* filter. An energy control strategy based on flatness properties is proposed. The system is proved to be flat; this strategy involves the global stability of the whole system at any operating conditions. The planed energy reference trajectories have been designed to respect the power supply constraints. The requirements of minimizing the

circulating current and balancing the currents between the parallel inverters are introduced to the parallel system with a nonlinear current balancing regulator. The experimental results show the validity of the proposed FBC method for regulating the output ac bus voltages and minimizing the circulating currents; the flatness property allows reducing the transient effects due to change of the configurations after fault detection.

REFERENCES

[1] H. Mahmood, D. Michaelson, and J. Jiang, "Accurate reactive power sharing in an islanded microgrid using adaptive virtual impedances," *IEEE Trans. Power Electron*., vol. 30, no. 3, pp. 1605–1617, Mar. 2015.

[2] F. Wang, Y. Wang, Q. Gao, C. Wang, and Y. Liu, "A control strategy for suppressing circulating currents in parallel-connected PMSM drives with individual DC links," *IEEE Trans. Power Electron.*, vol. 31, no. 2, pp. 1680–1691, Feb. 2016.

[3] X. Wang, F. Blaabjerg, M. Liserre, Z. Chen, J. He, and Y. W. Li, "An active damper for stabilizing power-electronics-based AC systems," *IEEE Trans. Power Electron.*, vol. 29, no. 7, pp. 3318–3329, Jul. 2014.

[4] J. Wang, N. Chang, X. Feng, and A. Monti, "Design of a generalized control algorithm for parallel inverters for smooth microgrid transition operation," *IEEE Trans. Ind. Electron.*, vol. 62, no. 8, pp. 4900–4914, Aug. 2015.

[5] X. Yu and A. M. Khambadkone, "Reliability analysis and cost optimization of parallel-inverter system," *IEEE Trans. Ind. Electron.*, vol. 59, no. 10, pp. 3881–3889, Oct. 2012.

[6] M. Abusara and S. M. Sharkh, "Design and control of a grid-connected interleaved inverter," *IEEE Trans. Power Electron.*, vol. 28, no. 2, pp. 748–764, Feb. 2013.

[7] Z. Shao, X. Zhang, F. Wang, and R. Cao, "Modeling and elimination of zero-sequence circulating currents in parallel three-level t-type grid-connected inverters," *IEEE Trans. Power Electron.*, vol. 30, no. 2, pp. 1050–1063, Feb. 2015.

[8] H. Renaudineau, A. Houari, A. Shahin, J.-P. Martin, S. Pierfederici, F. Meibody-Tabar, and B. Gerardin, "Efficiency optimization through current-sharing for paralleled DC–DC boost converters with parameter estimation," *IEEE Trans. Power Electron.*, vol. 29, no. 2, pp. 759–767, Feb. 2014.

[9] W. Lu, K. Zhou, D. Wang, and M. Cheng, "A general parallel structure repetitive control scheme for multiphase DC–AC PWM converters," *IEEE Trans. Power Electron.*, vol. 28, no. 8, pp. 3980–3987, Aug. 2013.

[10] Y. Zhang, M. Yu, F. Liu, and Y. Kang, "Instantaneous current-sharing control strategy for parallel operation of UPS modules using virtual impedance," *IEEE Trans. Power Electron.*, vol. 28, no. 1, pp. 432–440, Jan. 2013.

[11] B. B. Johnson, S. V. Dhople, A. O. Hamadeh, and P. T. Krein, "Synchronization of parallel single-phase inverters with virtual oscillator control," *IEEE Trans. Power Electron.*, vol. 29, no. 11, pp. 6124–6138, Nov. 2014.

[12] D. Meneses, O. Garcia, P. Alou, J. A. Oliver, and J. A. Cobos, "Grid-connected forward microinverter with primary-parallel secondary-series transformer," *IEEE Trans. Power Electron.*, vol. 30, no. 9, pp. 4819–4830, Sep. 2015.

[13] B. M. H. Jassim, D. J. Atkinson, and B. Zahawi, "Modular current sharing control scheme for parallel-connected converters," *IEEE Trans. Ind. Electron.*, vol. 62, no. 2, pp. 887–897, Feb. 2015.

[14] M. Narimani and G. Moschopoulos, "Three-phase multimodule VSIs using SHE-PWM to reduce zero-sequence circulating current," *IEEE Trans. Ind. Electron.*, vol. 61, no. 4, pp. 1659–1668, Apr. 2014.

[15] T.-P. Chen, "Zero-sequence circulating current reduction method for parallel HEPWM inverters between AC bus and DC bus," *IEEE Trans. Ind. Electron.*, vol. 59, no. 1, pp. 290–300, Jan. 2012.

[16] M.-J. Tsai and P.-T. Cheng, "Circulating current reduction of parallel connected four-pole inverters," in *Proc. 9th Int. Conf. Power Electron. ECCE Asia*, 2015, pp. 405–412.

[17] Z. Xueguang, C. Jiaming, M. Yan, W. Yijie, and X. Dianguo, "Bandwidth expansion method for circulating current control in parallel three-phase PWM converter connection system," *IEEE Trans. Power Electron.*, vol. 29, no. 12, pp. 6847–6856, Dec. 2014.

[18] Z. Xueguang, C. Jiaming, Z. Wenjie, and X. Dianguo, "Dual updating SVPWM-based circulating current control method for parallel three-phase inverters," in *Proc. 39th Annu. Conf. IEEE Ind. Electron. Soc.*, Nov. 10–13, 2013, pp. 659–664.

[19] H. Ma, Z. Lin, L. Dong, and Q. Guo, "Modeling and analysis of switching frequency circulating current in three-phase parallel inverters," in *Proc. IEEE 23rd Int. Symp. Ind. Electron.*, 2014, pp. 568–573.

[20] D. Zhang, F. Wang, R. Burgos and D. Boroyevich, "Common-mode circulating current control of paralleled interleaved three-phase two-level voltage-source converters with discontinuous space-vector modulation," *IEEE Trans. Power Electron.*, vol. 26, no. 12, pp. 3925–3935, Dec. 2011.

[21] T.-B. Lazzarin and I. Barbi, "DSP-based control for parallelism of three-phase voltage source inverter," *IEEE Trans. Ind. Informat.*, vol. 9, no. 2, pp. 749–759, May 2013.

[22] B. Zhao, Q. Song, W. Liu, and Y. Sun, "Overview of dual-active-bridge isolated bidirectional DC–DC converter for high-frequency-link power-conversion system," *IEEE Trans. Power Electron.*, vol. 29, no. 8, pp. 4091–4106, Aug. 2014.

[23] Y. Zhang, Y. Kang, and J. Chen, "The zero-sequence circulating currents between parallel three-phase inverters with three-pole transformers and reactors," in *Proc. 21st Annu. IEEE Appl. Power Electron. Conf. Expo.*, Mar. 2006. pp. 1709–1715.

[24] B. Cougo, T. Meynard, and G. Gateau, "Parallel three-Phase inverters: Optimal PWM method for flux reduction in intercell transformers," *IEEE Trans. Power Electron.*, vol. 26, no. 8, pp. 2184–2191, Aug. 2011.

[25] M. Narimani and G. Moschopoulos, "Improved method for paralleling reduced switch VSI modules: Harmonic content and circulating current," *IEEE Trans. Power Electron.*, vol. 29, no. 7, pp. 3308–3317, Jul. 2014.

[26] G. Gohil, R. Maheshwari, L. Bede, T. Kerekes, R. Teodorescu, M. Liserre, and F. Blaabjerg, "Modified discontinuous PWM for size reduction of the circulating current filter in parallel interleaved converters," *IEEE Trans. Power Electron.*, vol. 30, no. 7, pp. 3457–3470, Jul. 2015.

[27] D. J. Tschirhart and P. K. Jain, "Design procedure for high-frequency operation of the modified series-resonant APWM converter to reduce size and circulating current," *IEEE Trans. Power Electron.*, vol. 27, no. 10, pp. 4181–4191, Oct. 2012.

[28] J. Liu, X. Qin, H. Lin, and L. Bu, "Analysis on circulating current of parallel inverter with SPWM modulation for AC motor drive," in *Proc. Int. Conf. IEEE Model. Identification Control*, Jun. 2012, pp. 1080–1086.

[29] M. Fliess, J. Lévine, P. Martin, and P. Rouchon, "Flatness and defect of non-linear systems: Introductory theory and examples," *Int. J. Control*, vol. 61, no. 6, pp. 1327–1361, 1995.

[30] P. Martin, R. M. Murray, and P. Rouchon, "Flat systems," in *Proc. 4th Eur. Control Conf.*, Brussels, Belgium, 1997, pp. 211–264.

[31] A. Shahin, B. Huang, J.-P. Martin, S. Pierfederici, and B. Davat, "New non-linear control strategy for non-isolated DC/DC converter with high voltage ratio," *Energy Convers. Manage.*, vol. 51, no. 1, pp. 56–63, 2010.

[32] A. Shahin, M. Hinaje, J.P. Martin, S. Pierfederici, S. Raël, and B. Davat, "High voltage ratio DC–DC converter for fuel-cell applications," *IEEE Trans. Ind. Electron.*, vol. 57, no. 12, pp. 3944–955, Dec. 2010.

[33] A. Gensior, T. M. P. Nguyen, J. Rudolph, and H. Guldner, "Flatness-based loss optimization and control of a doubly fed induction generator system," *IEEE Trans. Control. Syst. Technol.*, vol. 19, no. 6, pp. 1457–1466, Nov. 2011.

[34] P. Thounthong, "Control of a three-level boost converter based on a differential flatness approach for fuel cell vehicle applications," *IEEE Trans. Veh. Technol.*, vol. 61, no. 3, pp. 1467–1472, Mar. 2012.

[35] M. Pahlevaninezhad, P. Das, J. Drobnik, P. K. Jain, and A. Bakhshai, "A new control approach based on the differential flatness theory for an AC/DC converter used in electric vehicles," *IEEE Trans. Power Electron.*, vol. 27, no. 4, pp. 2085–2103, Apr. 2012.

[36] A. Shahin, A. Payman, J.-P. Martin, S. Pierfederici, and F. Meibody-Tabar, "Approximate novel loss formulae estimation for optimization of power controller of DC–DC converter," in *Proc. 36th Annu. Conf. IEEE Ind. Electron. Soc.*, 2010, pp. 373–378.

[37] M. Hua, H. Hu, X. Xing, and J.-M. Guerrero, "Multilayer control for inverters in parallel operation without intercommunications," *IEEE Trans. Power Electron.*, vol. 27, no. 8, pp. 3651–3663, Aug. 2012.

[38] A. Houari, H. Renaudineau, J.-P. Martin, S. Pierfederici, and F. Meibody-Tabar, "Flatness based control of three phase inverter with output LC filter," *IEEE Trans. Ind. Electron.*, vol. 59, no. 7, pp 2890–2897, Jul. 2012.

[39] A. Shahin, J.-P. Martin, B. Nahid-Mobarakeh, and S. Pierfederici, "Optimal efficiency operation of non-isolated DC/DC converter for high voltage ratio applications," in *Proc. 36th Annu. Conf. IEEE Ind. Electron. Soc.*, 2013, pp. 1106–1111.

[40] A. Shahin, H. Moussa, H. Renaudineau, A. Houari, J.-P. Martin, B. Nahid-Mobarakeh, S. Pierfederici, and A. M. Sharaf, "Optimal efficiency optimization through power-sharing for paralleled DC-AC inverters with

parameters estimator," in *Proc. 11th Int. Conf. ELECTRIMACS*, 2014, pp. 463–468.
[41] G. Perez-Ladron, V. Cárdenas, and G. Espinosa, "Analysis and implementation of a master–slave control based on a passivity approach for parallel inverters operation," in *Proc. IEEE Int. Power Electron. Congr.*, 2006, pp. 1–5.
[42] M. Borrega, L. Marroyo, R. Gonzalez, J. Balda, and J. L. Agorreta, "Modeling and control of a master–slave PV inverter with N-paralleled inverters and three-phase three-limb inductors," *IEEE Trans. Power Electron.*, vol. 28, no. 6, pp. 2842–2855, Jun. 2013.
[43] Z. Liu, J. Liu, X. Hou, Q. Dou, D. Xue, and T. Liu, "Output impedance modeling and stability prediction of three-phase paralleled inverters with master–slave sharing scheme based on terminal characteristics of individual inverters," *IEEE Trans. Power Electron.*, vol. 31, no. 7, pp. 5306–5320, Jul. 2016.

Ahmed Shahin (M'08–SM'15) received the B.Sc. and M.Sc. degrees in electrical engineering from Mansoura University, Mansoura, Egypt, in 2000 and 2004, respectively, and the Ph.D. degree in electrical engineering from Ecole Nationale Supérieure d'electricité et de Mécanique, Université de Lorraine, Nancy, France, in 2011.

Since 2012, he has been a Doctoral Researcher at Mansoura University. His current research interests include renewable energy systems, modeling, optimization methods oriented to power flows management, control and diagnosis of photovoltaic power systems, and fault-tolerant power electronic systems.

Hassan Moussa (M'15) received the B.S. degree in electrical and electronic engineering from the Lebanese University, Beirut, Lebanon, in 2010, and the M.S. degree in renewable energies from the Lebanese University in collaboration with Saint-Joseph University, Beirut, in 2012. He is currently working toward the Ph.D. degree in electrical engineering at Lorraine University, Nancy, France.

His current research interests include renewable energy systems, distributed generation systems, microgrids, and power quality issues of electrical systems.

Ivano Forrisi was born in Vallo della Lucania, Italy, in 1987. He received the M.Sc. degree in electronic engineering from the University of Salerno, Fisciano, Italy, in 2013. He is currently working toward the Ph.D. degree at the Ecole Nationale Supérieure d'Electricité et de Mécanique, Groupe de Recherche en Electrotechnique et Electronique de Nancy, Nancy, France.

His main research interests include modeling, control, and large signal stability study of dc/dc and dc/ac converters for renewable energy applications.

Jean-Philippe Martin graduated from the University of Nancy, Nancy, France. He received the Ph.D. degree from the Institut National Polytechnique de Lorraine, Vandoeuvre-les-Nancy, France, in 2003.

Since 2004, he has been an Assistant Professor at the Institut National Polytechnique de Lorraine. His research activities in the Groupe de Recherche en Electrotechnique et Electronique de Nancy, Nancy, UMR/CNRS, include electrical machine controls, static converter architectures, and their interactions with new electrical devices (fuel cell and photovoltaic system).

Babak Nahid-Mobarakeh (M'05–SM'12) received the Ph.D. degree in electrical engineering from the Institut National Polytechnique de Lorraine, Nancy, France, in 2001.

From 2001 to 2006, he was an Assistant Professor with the Centre de Robotique, Electrotechnique et Automatique, University of Picardie, Amiens, France. In September 2006, he joined the Ecole Nationale Superieure d'Electricite et de Mecanique, Université de Lorraine, Nancy, where he is currently an Associate Professor. He is also with the Groupe de Recherche en Electrotechnique et Electronique de Nancy, Nancy. He is the author or coauthor of more than 150 international peer-reviewed journal and conference papers. His main research interests include nonlinear and robust control techniques applied to electric systems, fault detection and fault-tolerant control of power converters and drives, power management, and stabilization of microgrids.

Dr. Nahid-Mobarakeh is the Chair of the Industrial Automation and Control Committee of the IEEE Industry Applications Society.

Serge Pierfederici received the Engineer degree from the École Nationale Supérieure en Électricité et Mécanique, Nancy, France, in 1994, and the Ph.D. degree in electrical engineering and the Habilitation à Diriger des Recherches degree from the Institut National Polytechnique de Lorraine, Nancy, in 1998 and 2007, respectively.

Since 2009, he has been a Professor with the Université de Lorraine, Nancy. His research interests include stability study of distributed power systems and modeling and control of power electronic converters.